# AIRBORNE MEASUREMENTS OF ATOMIC DEBRIS

*By L. Machta, H. L. Hamilton, Jr., L. F. Hubert, R. J. List, and K. M. Nagler*

U. S. Weather Bureau

(Manuscript received 2 September 1956)

ABSTRACT

The primary purpose of this article is the documentation of radioactivity data collected by airborne equipment during the first of the Nevada atomic tests. While absolute magnitudes of activity are not available, the relative values are useful in checking meteorological trajectories and in making crude estimates of lateral diffusion.

## 1. Introduction

The usefulness of atomic debris as a tracer for meteorological experiments results from the ability of physicists to monitor the amount of radioactivity over a very wide range and to great distances, and from the availability of the material in large quantities during tests of atomic devices in Nevada. In a previous report, List [1] showed the distribution of the deposited debris over the United States following several of the spring 1952 atomic tests in Nevada. The present article will describe and illustrate similar observations of the atomic debris made by aircraft. The advantage of aircraft measurements is twofold: first, the magnitude of the deposited debris depends on the presence of a mechanism to deposit the particles and is therefore not necessarily a measure of the air concentration, while the airborne equipment specifically measures the air concentration; and second, the ground sampling is made at stations several hundreds of miles apart, while the airborne equipment can provide a continuous profile over a long distance.

In general, flights were made along the 80th and 95th meridians, at elevations between 8000 and 30,000 ft. The aircraft were equipped with two filters, identified as "left" and "right." The filters were changed alternately every 15 min, so that each filter was exposed for 30-min periods. After sufficient time for decay of the natural radioactivity, the filter was measured with a Geiger counter. The conversion of the activity into disintegrations per minute, or curies per unit volume of air, was not attempted due to inadequate information on the efficiency of the filter, the counting geometry of the Geiger counters, *etc.* It is only possible to treat the radioactivity collected on the filters on a *relative* basis. For practical purposes, all observations reported at different places and at different elevations may be directly compared.

TABLE 1. List of bursts in Operation RANGER.

| Burst number | Date | Time (GCT) | Approximate maximum altitude (feet msl) |
|---|---|---|---|
| 1 | 27 January 1951 | 1345 | 17,000 |
| 2 | 28 January 1951 | 1350 | 35,000 |
| 3 | 1 February 1951 | 1415 | 12,000 |
| 4 | 2 February 1951 | 1345 | 35,000 |
| 5 | 6 February 1951 | 1347 | 40,000 |

## 2. Measurements during Operation RANGER

The observations reported in this article were made during the Nevada tests conducted by the Atomic Energy Commission during January and February 1951 (Operation RANGER). Table 1 shows the dates on which the detonations occurred and the approximate heights of the tops of the atomic clouds.

Figs. 1 through 5 show the meteorological trajectories prepared at the U. S. Weather Bureau with use of the observed winds. Standard constant-pressure charts formed the basis for most of the trajectories; but at a few levels between the regular charts, winds were analyzed on constant-level surfaces. The trajectories are identified by heights, such that 10,000 ft corresponds to 700 mb, 18,000 ft to 500 mb, 24,000 ft to 400 mb, 30,000 ft to 300 mb, and 40,000 ft to 200 mb. Observed winds, whenever available, were used in preference to the geostrophic winds, and 6-hr charts were prepared to reduce the interval over which the time interpolation was required. 700-mb trajectories were abandoned in many cases where the air flow over the mountains was too uncertain.

Figs. 6 through 48 show the profiles along the 80th and 95th meridians. The ordinate represents the relative activity per 30 min of flight — no particular significance can be attached to the absolute values of the numbers, as noted earlier. The ordinate is plotted on a logarithmic scale (except for one case, fig. 11), because of the large range of values. The abscissa is a plot of latitude on a linear scale. The dates and times of the two extreme filters are given, as well as the altitude and flight line. On some figures, the position of the meteorological trajectory is shown by

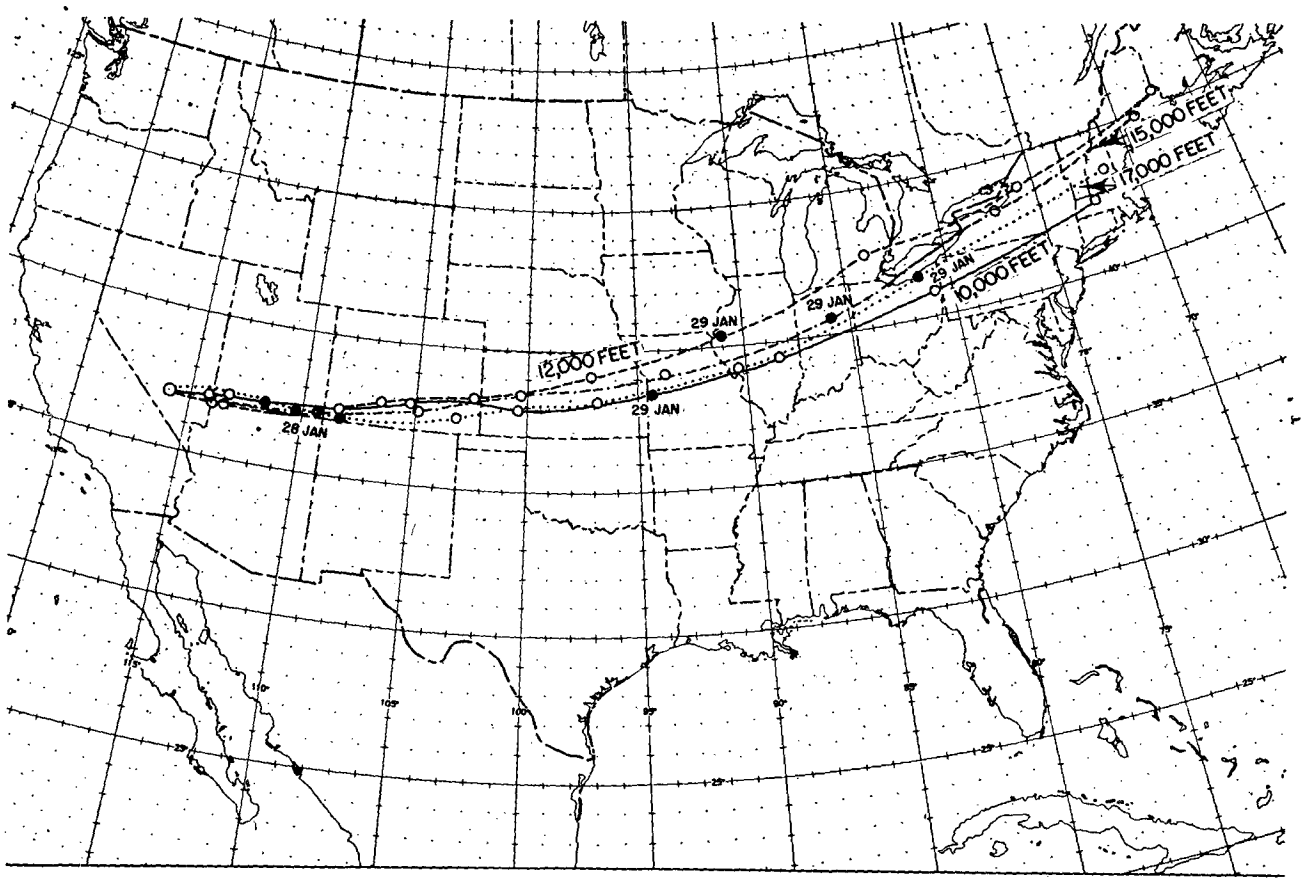


FIG. 1. Meteorological trajectories for burst 1, 1345 GCT 27 January 1951. (Circles indicate 6-hr positions. Solid circles represent 0000 GCT on date indicated.)

a vertical arrow. As with any type of new measurement, many errors of observation are present in the data. Inconsistencies are evident — cases where successive filters on one side indicate high activity and the overlapping filter on the other side records negligible activity. Part of the irregularities must be the result of the particulate nature of the debris and some due to slight differences in the characteristics of the filters. It is the writers' opinion that most of the patterns, however, represent real distributions of radioactivity. Figs. 49 and 50 show two special flights made across the Gulf of Mexico.

### 3. Trajectory errors

Table 2 shows the errors which were made in the after-the-fact trajectories of figs. 1 to 5 for profiles made within a reasonable time after the passage of the meteorological trajectory. The latitude at which the meteorological trajectory crossed the flight line is compared with the best estimate of the latitude of the peak concentration as made from the activity profiles. Several cautions must be exercised in the interpretation of the results. First, the errors in the last column represent only the cross-wind errors and not the total errors. On the assumption that the errors are equal in all directions, one might multiply them by $2\frac{1}{2}$. However, other experience suggests that the errors in the direction of the flow are likely to be greater than the cross-wind errors. Second, a case was selected only if the trajectory was reasonably verified, so that one could be sure of following the correct atomic cloud. Thus, a few cases of very bad

TABLE 2. Comparison of observed peak concentrations with meteorological trajectories.

| Activity profile | Date | Time (GCT) | Latitude (deg N) | Longitude (deg W) | Altitude (feet) | Latitudinal distance from meteorological trajectory (deg lat) |
|---|---|---|---|---|---|---|
| Fig. 7 | Jan. 28 | 1730 | 39.3 | 95 | 16,000 | 0.4 |
| Fig. 8 | Jan. 28 | 2000 | 38.7 | 95 | 14,000 | 0.2 |
| Fig. 10 | Jan. 29 | 0330 | 39.2 | 95 | 9,000 | 0.8 |
| Fig. 14 | Jan. 29 | 1830 | 39.8 | 95 | 10,000 | 1.0 |
| Fig. 12 | Jan. 29 | 2200 | 39.0 | 95 | 24,000 | 1.3 |
| Fig. 32 | Feb. 4 | 0300 | 27.3 | 95 | 16,000 | 0.5 |
| Fig. 33 | Feb. 4 | 0845 | 25.8 | 95 | 11,000 | 0.2 |
| Fig. 26 | Feb. 4 | 1200 | 26.5 | 95 | 8,000 | 0.9 |
| Fig. 35 | Feb. 7 | 1845 | 29.6 | 95 | 30,000 | 2.6 |
| Fig. 40 | Feb. 8 | 0915 | 26.6 | 95 | 18,000 | 1.1 |
| Fig. 39 | Feb. 8 | 1300 | 26.0 | 95 | 16,000 | 0.5 |
| Fig. 37 | Feb. 8 | 2000 | 24.2 | 95 | 14,000* | 1.2 |
| Fig. 49 | Feb. 8 | 2145 | 23.7 | 84.8 | 18,000 | 1.5 |
| | | | | | Mean: | 0.94 |

* Compared with 18,000-ft trajectory.

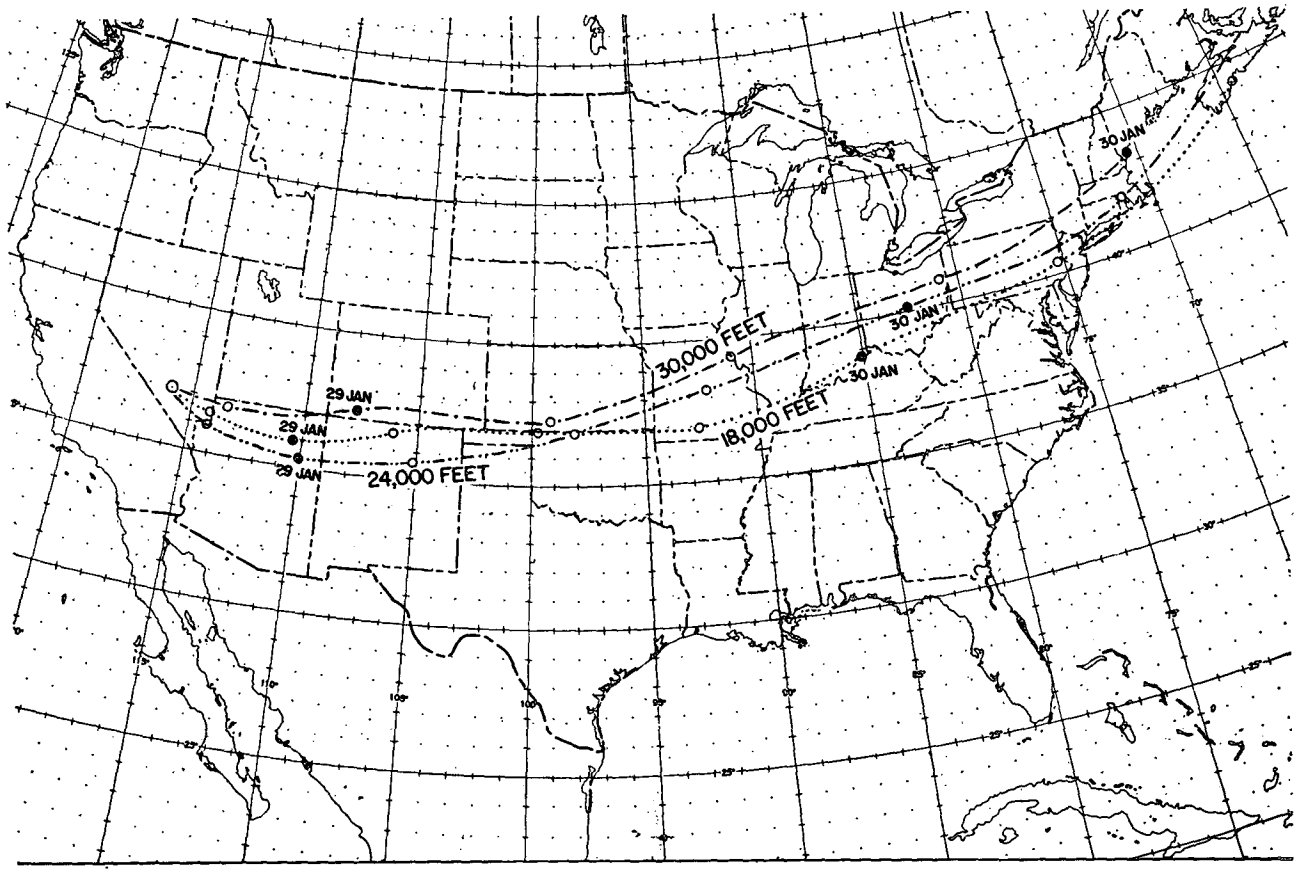


FIG. 2. Meteorological trajectories for burst 2, 1350 GCT 28 January 1951.

errors were omitted. One might also add that only those cases were chosen for which the flight altitude was within 2000 ft of height of the trajectory, but this does not bias the data.

The errors noted in table 2 tend to be considerably smaller than those in comparable after-the-fact trajectories verified by balloons as, for example, by Moore *et al* [2]. Not all of the differences can be attributed to the limitations noted in the above paragraph, nor is it felt that they are due to the fact that the balloons are affected more by eddy motion.[1] Rather, it is the writers' opinion that trajectories can be made more accurately for lower levels, where more wind observations are available. It will be noted that, in general, the larger errors in table 2 are at the upper levels (18,000 to 30,000 ft), and it was at 30,000 ft that the balloon flights were made.

The debris from atomic tests is probably concentrated initially in the mushroom portion of the stabilized atomic cloud, which is from 5000 to 15,000 ft thick, on the average. Particles are presumed to be of varying sizes immediately following the explosion; but by the time the cloud reaches the flight lines, most of the particles in excess of, perhaps, 10 $\mu$ in

[1] That is, the balloon represents only one particle. The atomic cloud, being composed of many particles, in effect cancels out the eddy motion, since we can deal with the peak concentration.

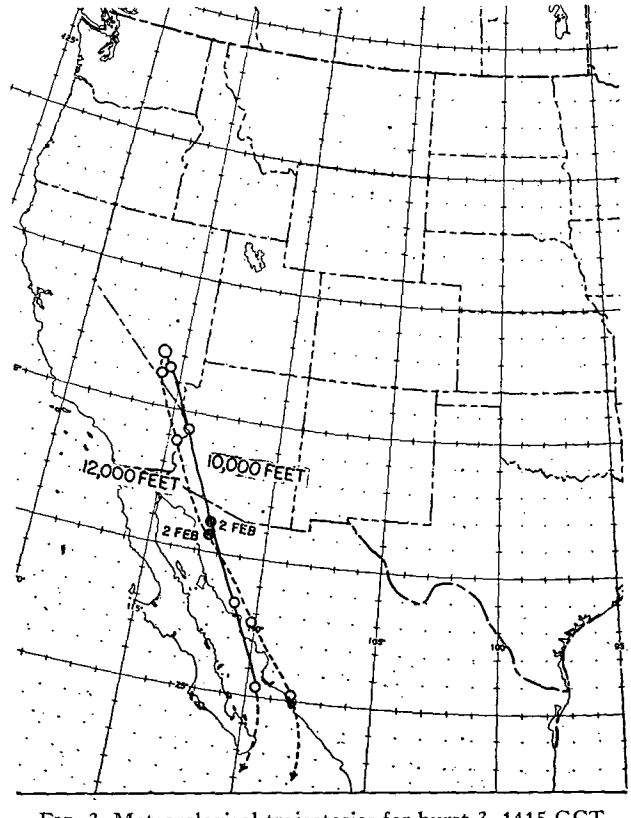


FIG. 3. Meteorological trajectories for burst 3, 1415 GCT 1 February 1951.

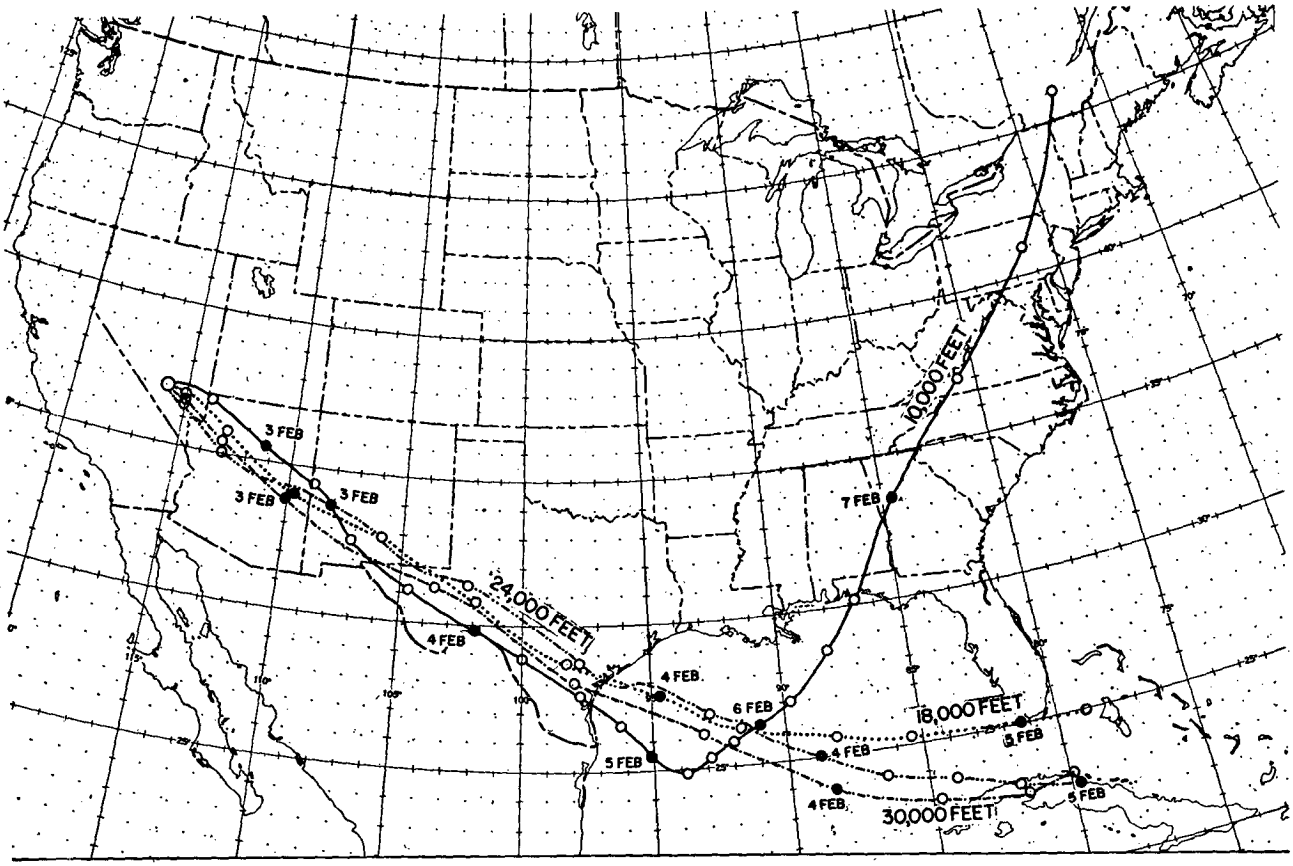


FIG. 4. Meteorological trajectories for burst 4, 1345 GCT 2 February 1951.

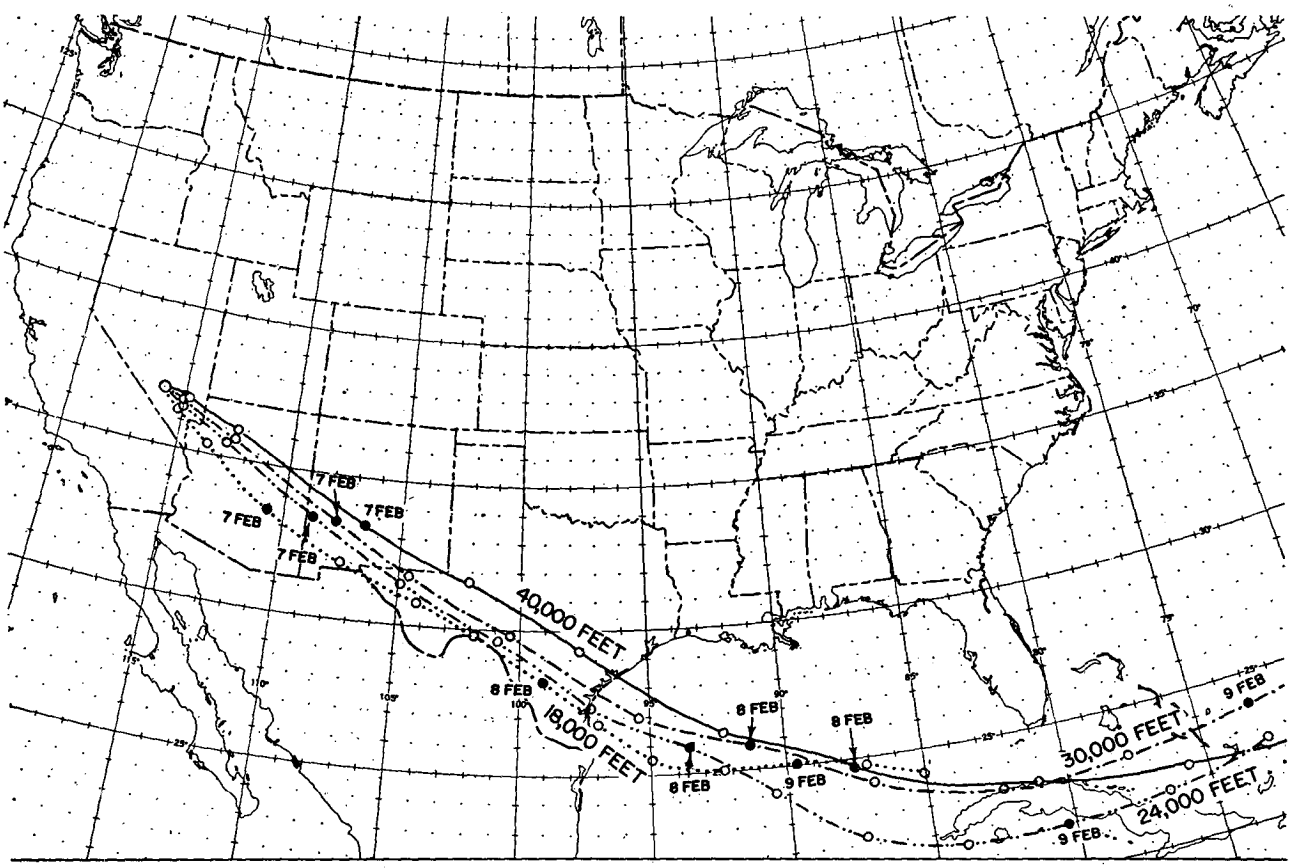


FIG. 5. Meteorological trajectories for burst 5, 1347 GCT 6 February 1951.

diameter have fallen to the ground. The remaining particles have very small fall velocities in comparison with the vertical motions of the atmosphere, and the main transport is believed to result from the flux due to diffusion rather than from gravitational settling. The lack of starting with a point source, added to the complications of vertical diffusion and shear and of horizontal diffusion and transport, gives rise to the irregular patterns which figs. 6 through 50 exhibit. The presence of debris from preceding atomic clouds occasionally adds to the confusion.

### 4. Apparent diffusion coefficients

Three profiles which provided pictures as might be expected from simple lateral diffusion alone were investigated. On the assumption that the lateral spread resulted exclusively from horizontal mixing and that the classical Fickian law of diffusion was applicable, the coefficient of lateral eddy mixing was found to be in the range from 1.6 to 4.8 $\times$ $10^8$ cm$^2$/sec.

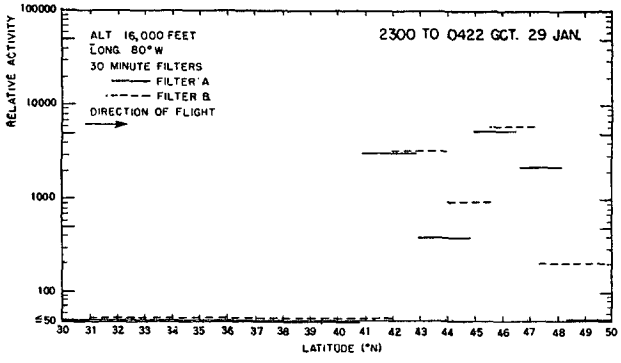


FIG. 6. Radioactivity profile, 29 January 1951, 16,000 ft. (Solid and dashed lines show relative activity measured on "right" and "left" filters, respectively. Lengths of lines indicate latitude traversed during exposure. Times of insertion of first filter and of removal of last filter are given.)

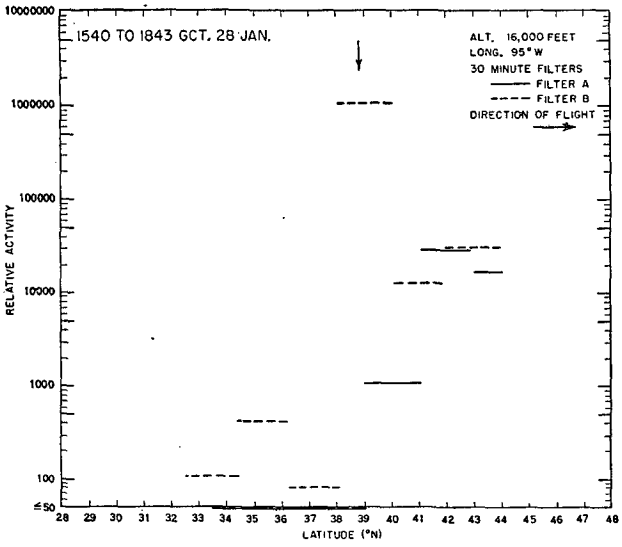


FIG. 7. Radioactivity profile, 28 January 1951, 16,000 ft.

The spread of balloons, travelling about as great distances as did the atomic debris to the flight lines, yielded coefficients of horizontal eddy diffusion (total, not lateral) equal to about 4 $\times$ $10^7$ cm$^2$/sec, according to Moore *et al* [2]. The number of cases upon which both of these coefficients of diffusion are based is certainly too small to deduce any far-reaching conclusions; but there is a suggestion that the three-dimensional nature of the debris, permitting the vertical wind shears to act, may be the cause of the difference. The coefficient of eddy diffusion determined from the atomic debris thus represents an "effective" coefficient which includes some mechanisms not described by Fickian diffusion. In any case, atomic debris and balloon pairs represent the best means presently available of measuring diffusion to the indicated distance.

Figs. 6 through 50 probably give a false impression of the cloud width, since the figures are plotted on a logarithmic scale. Fig. 11 is a repetition of fig. 10, plotted on a linear scale of activity, and shows the relatively narrow nature of the cloud.

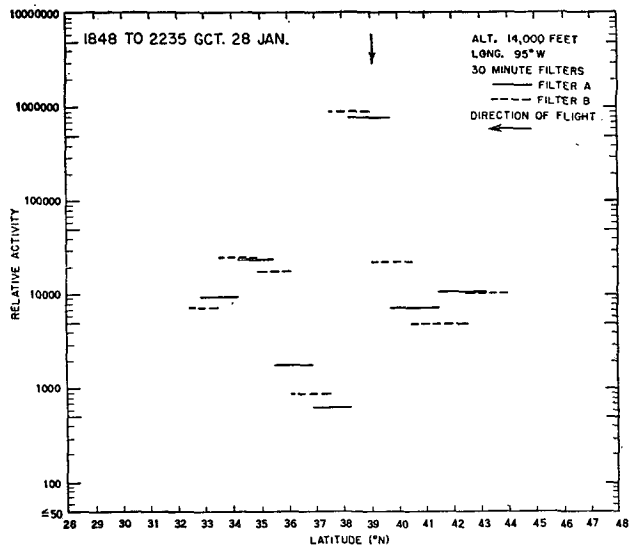


FIG. 8. Radioactivity profile, 28 January 1951, 14,000 ft.

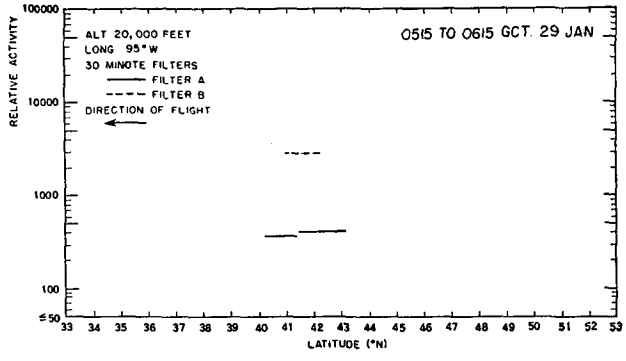


FIG. 9. Radioactivity profile, 29 January 1951, 20,000 ft.

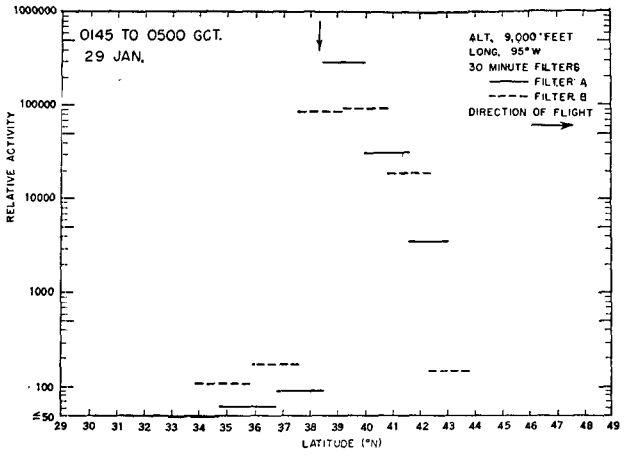


FIG. 10. Radioactivity profile, 29 January 1951, 9000 ft.

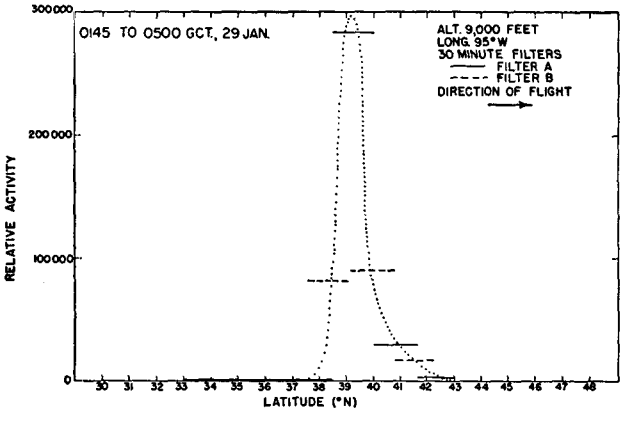


FIG. 11. Radioactivity profile, 29 January 1951, 9000 ft. (Linear scale.)

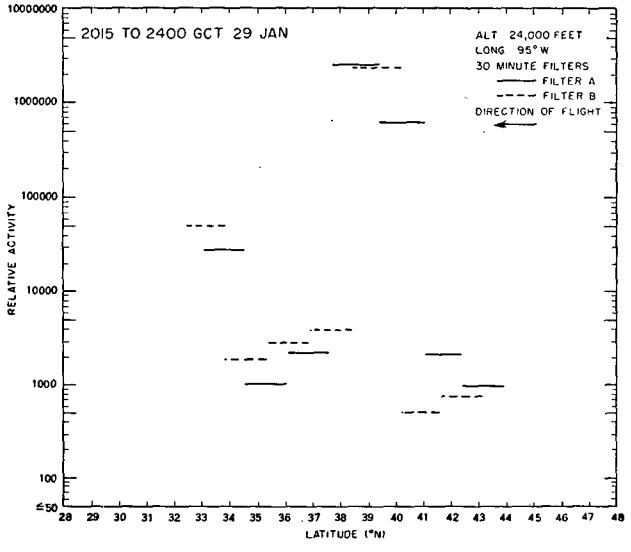


FIG. 12. Radioactivity profile, 29 January 1951, 24,000 ft.

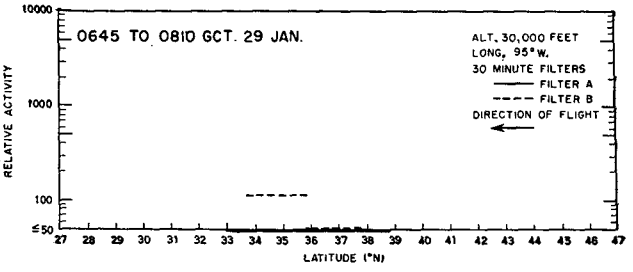


FIG. 13. Radioactivity profile, 29 January 1951, 30,000 ft.

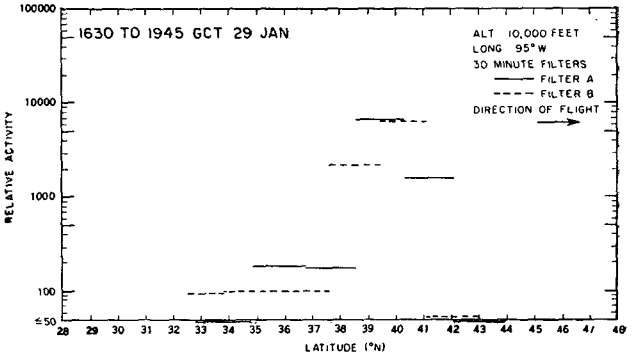


FIG. 14. Radioactivity profile, 29 January 1951, 10,000 ft.

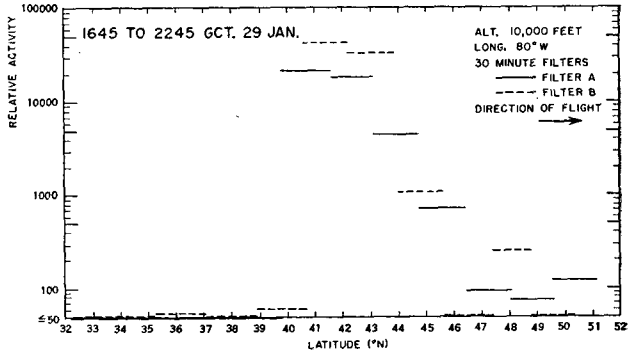


FIG. 15. Radioactivity profile, 29 January 1951, 10,000 ft.

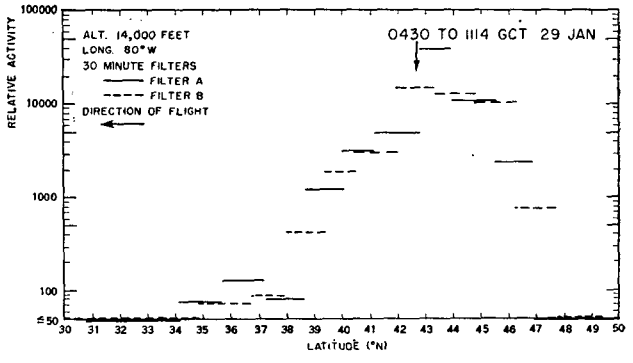


FIG. 16. Radioactivity profile, 29 January 1951, 14,000 ft.

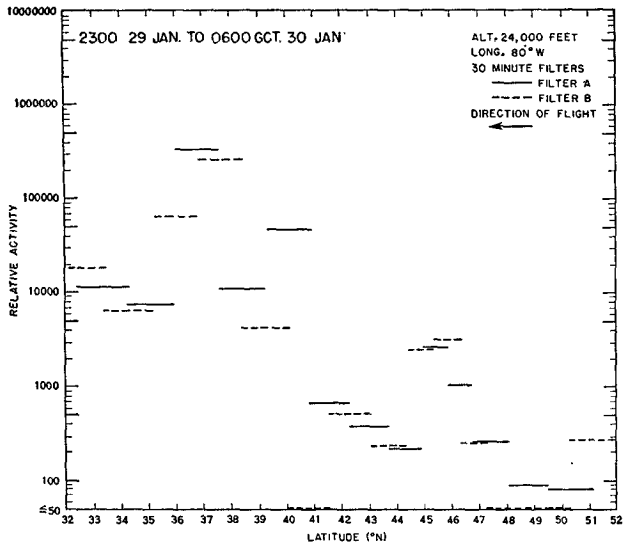


FIG. 17. Radioactivity profile, 30 January 1951, 24,000 ft.

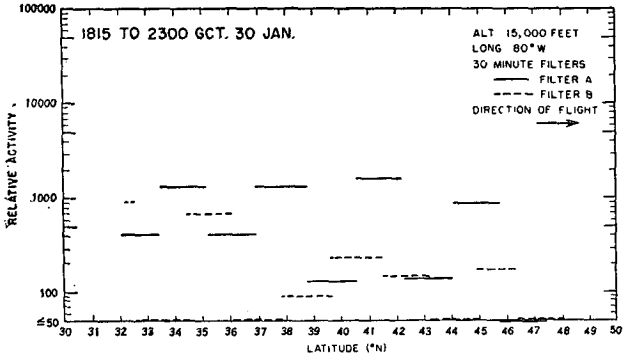


FIG. 18. Radioactivity profile, 30 January 1951, 15,000 ft.

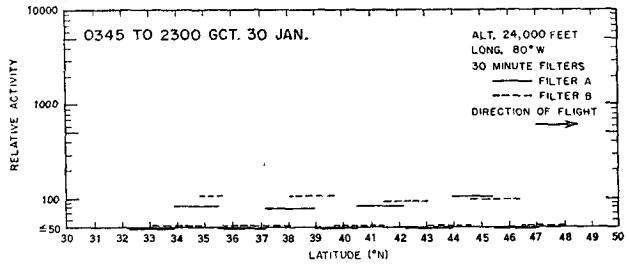


FIG. 19. Radioactivity profile, 30 January 1951, 24,000 ft.

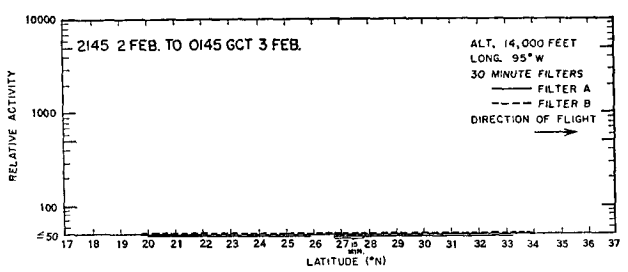


FIG. 20. Radioactivity profile, 3 February 1951, 14,000 ft.

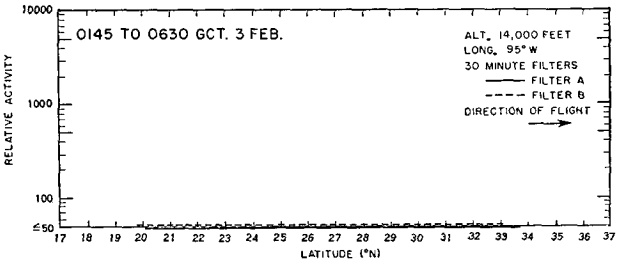


FIG. 21. Radioactivity profile, 3 February 1951, 14,000 ft.

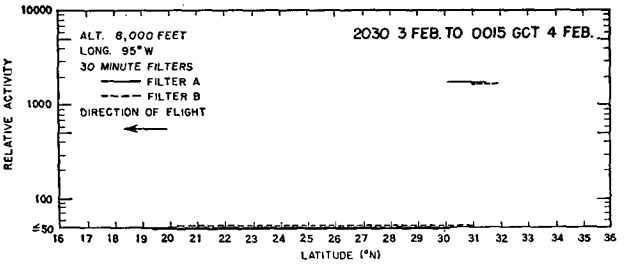


FIG. 22. Radioactivity profile, 3 February 1951, 8000 ft.

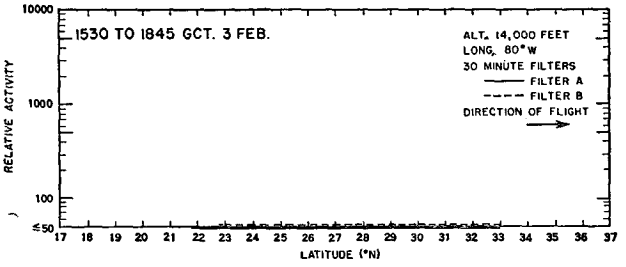


FIG. 23. Radioactivity profile, 3 February 1951, 14,000 ft.

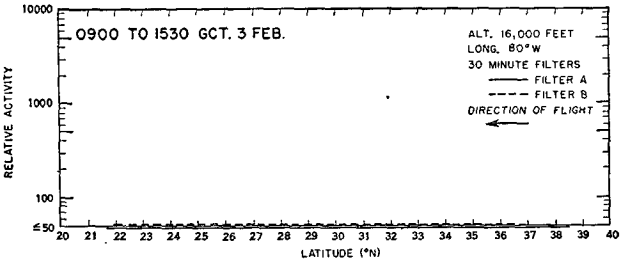


FIG. 24. Radioactivity profile, 3 February 1951, 16,000 ft.

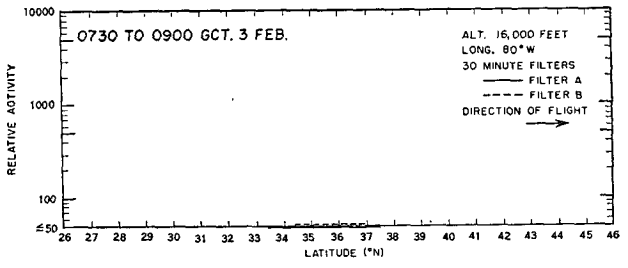


FIG. 25. Radioactivity profile, 3 February 1951, 16,000 ft.

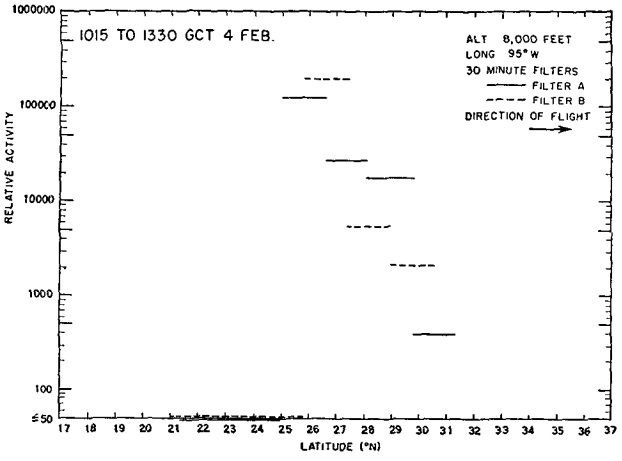


FIG. 26. Radioactivity profile, 4 February 1951, 8000 ft.

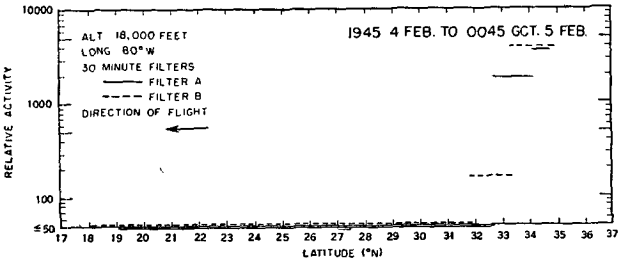


FIG. 27. Radioactivity profile, 5 February 1951, 18,000 ft.

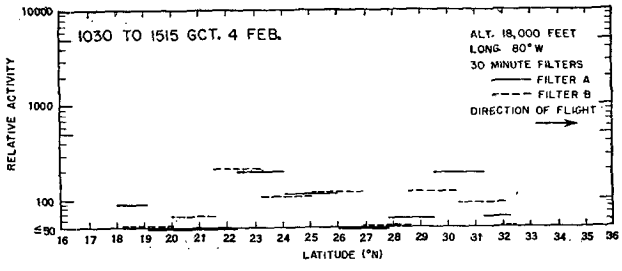


FIG. 28. Radioactivity profile, 4 February 1951, 18,000 ft.

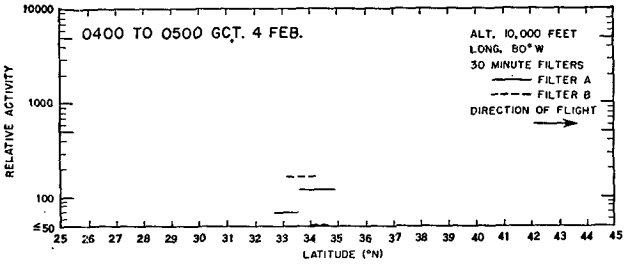


FIG. 29. Radioactivity profile, 4 February 1951, 10,000 ft.

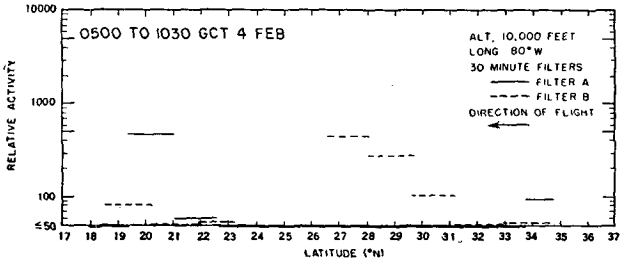


FIG. 30. Radioactivity profile, 4 February 1951, 10,000 ft.

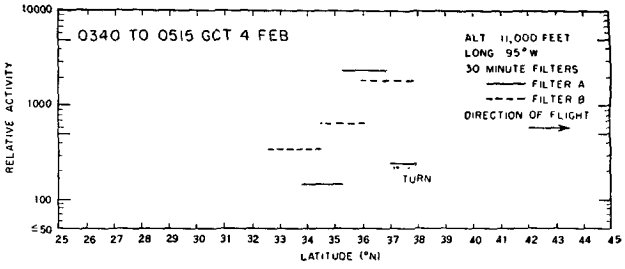


FIG. 31. Radioactivity profile, 4 February 1951, 11,000 ft.

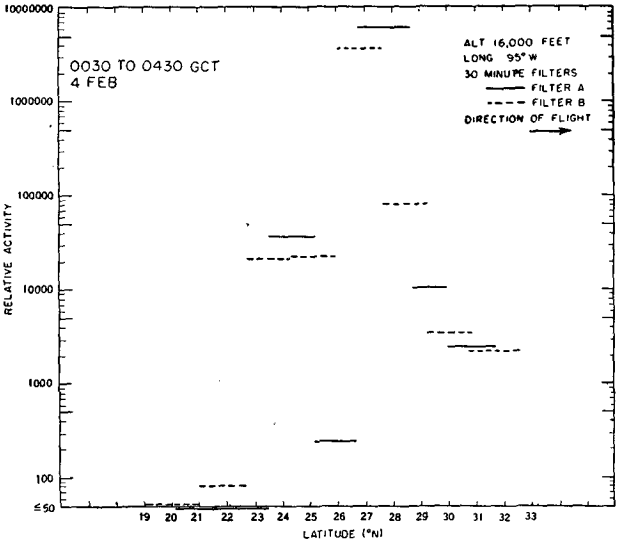


FIG. 32. Radioactivity profile, 4 February 1951, 16,000 ft.

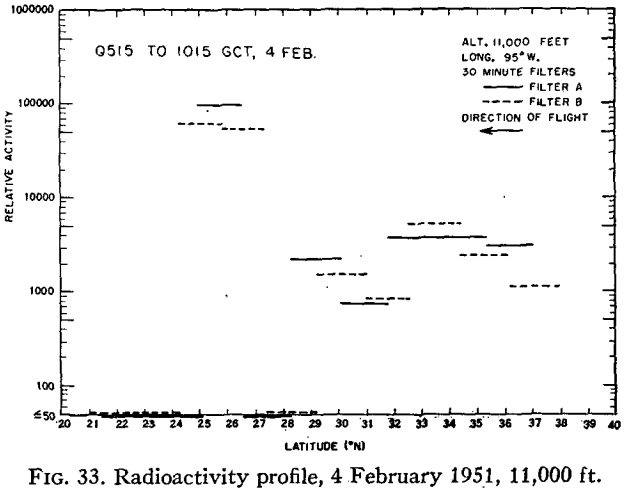


FIG. 33. Radioactivity profile, 4 February 1951, 11,000 ft.

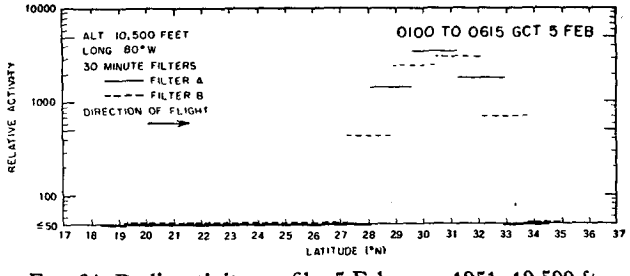


FIG. 34. Radioactivity profile, 5 February 1951, 10,500 ft.

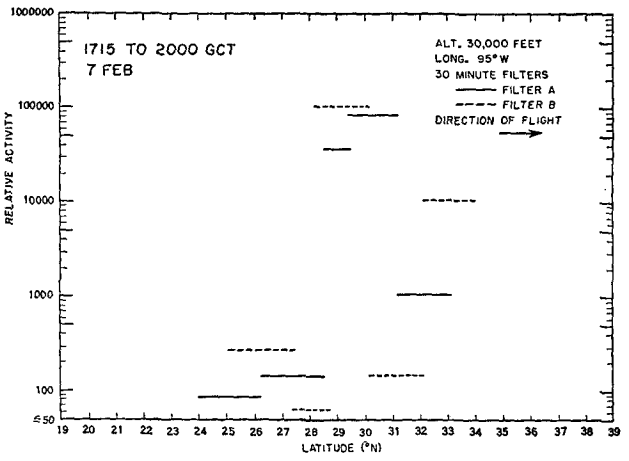


FIG. 35. Radioactivity profile, 7 February 1951, 30,000 ft.

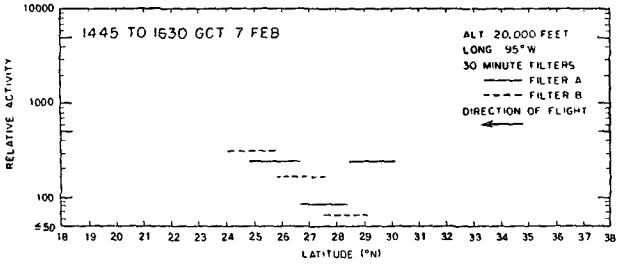


FIG. 36. Radioactivity profile, 7 February 1951, 20,000 ft.

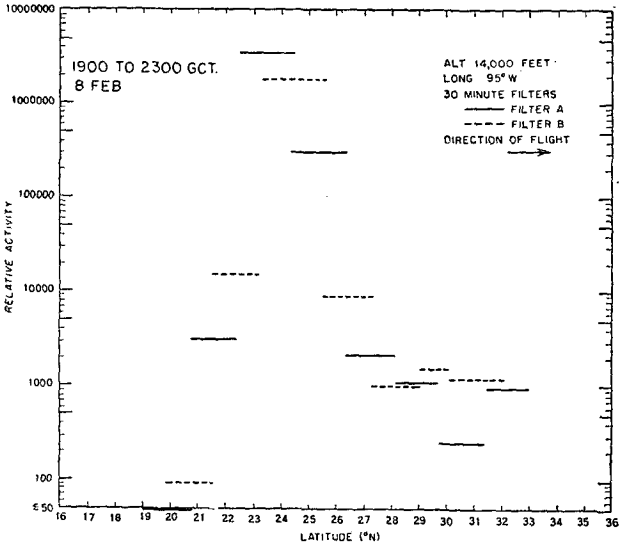


FIG. 37. Radioactivity profile, 8 February 1951, 14,000 ft.

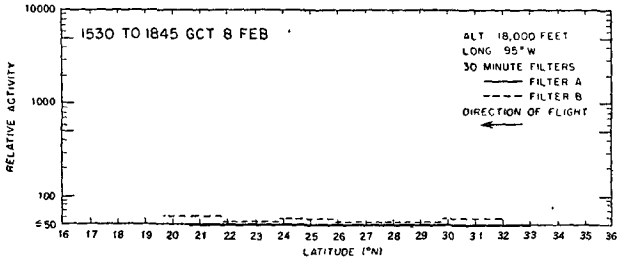


FIG. 38. Radioactivity profile, 8 February 1951, 18,000 ft.

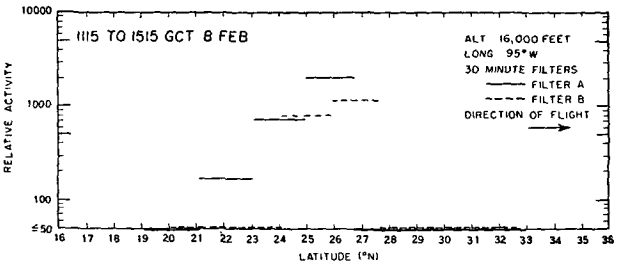


FIG. 39. Radioactivity profile, 8 February 1951, 16,000 ft.

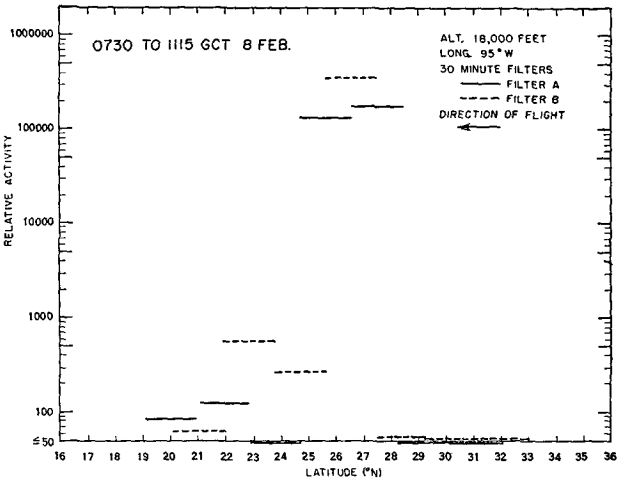


FIG. 40. Radioactivity profile, 8 February 1951, 18,000 ft.

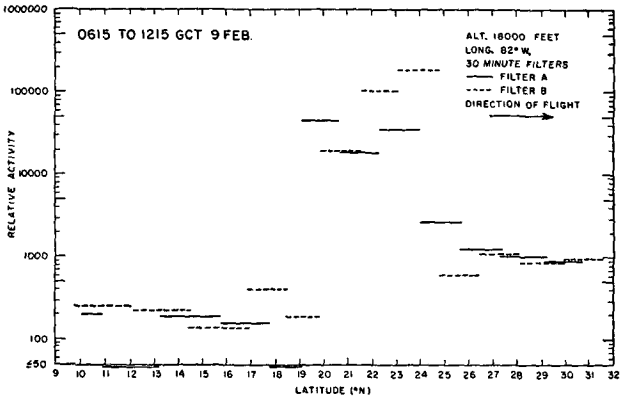


FIG. 41. Radioactivity profile, 9 February 1951, 18,000 ft.

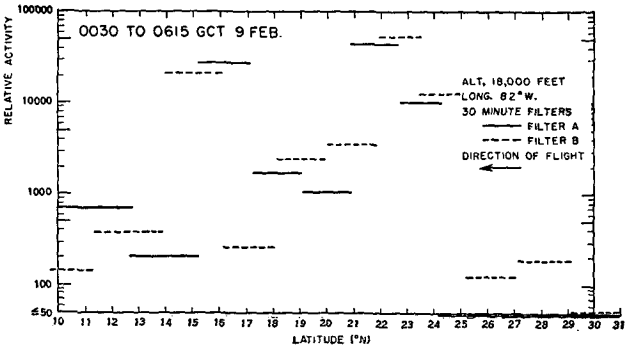


FIG. 42. Radioactivity profile, 9 February 1951, 18,000 ft.

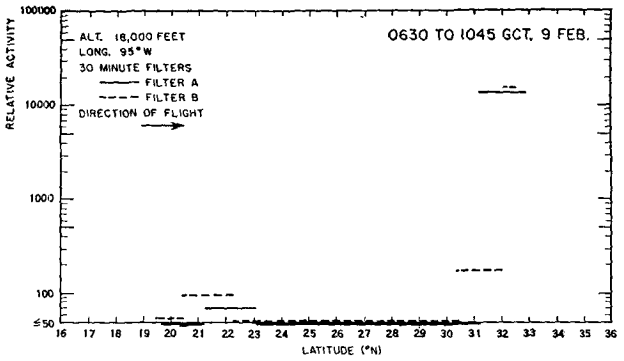


FIG. 43. Radioactivity profile, 9 February 1951, 18,000 ft.

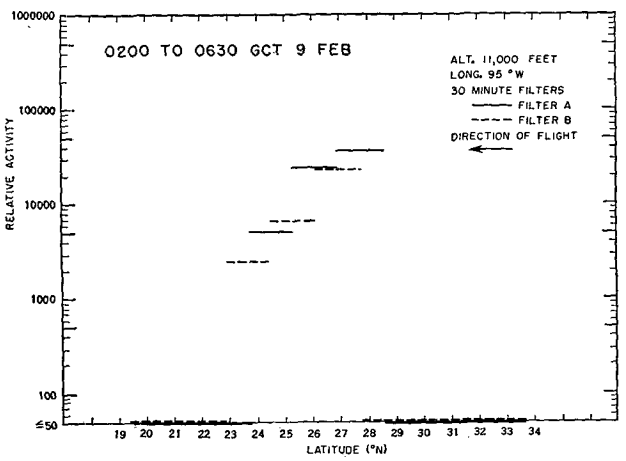


FIG. 44. Radioactivity profile, 9 February 1951, 11,000 ft.

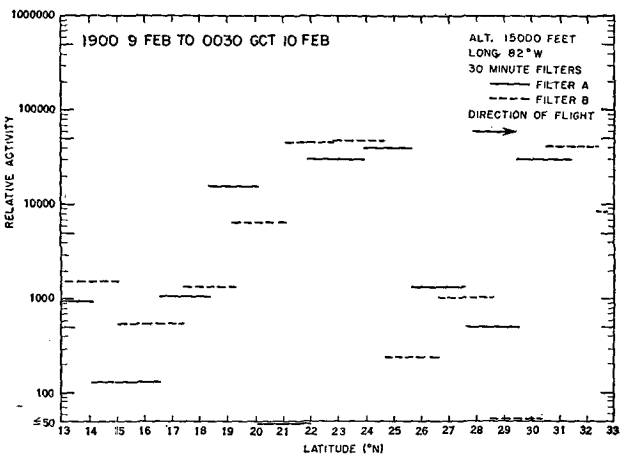


FIG. 45. Radioactivity profile, 10 February 1951, 15,000 ft.

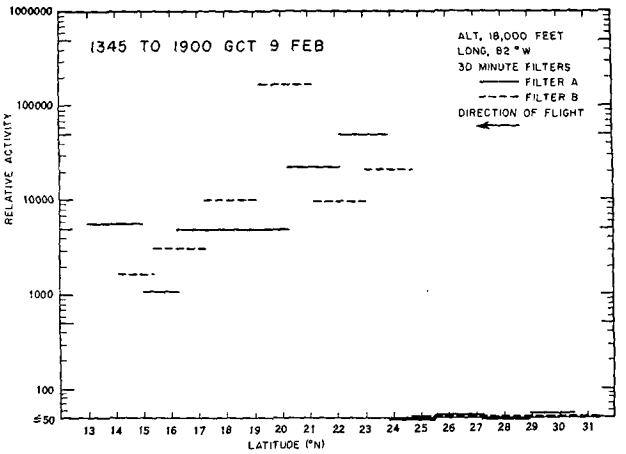


FIG. 46. Radioactivity profile, 9 February 1951, 18,000 ft.

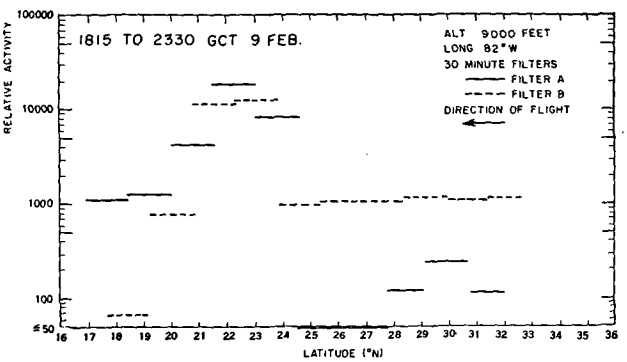


FIG. 47. Radioactivity profile, 9 February 1951, 9000 ft.

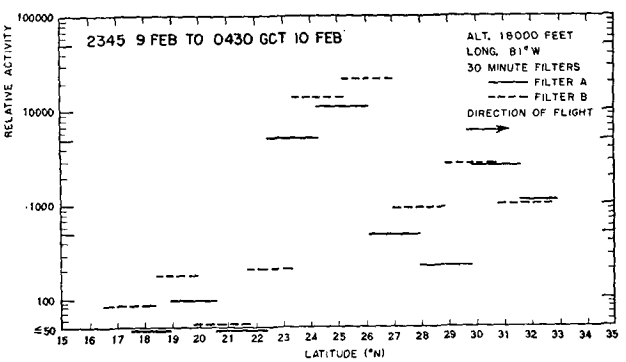


FIG. 48. Radioactivity profile, 10 February 1951, 18,000 ft.

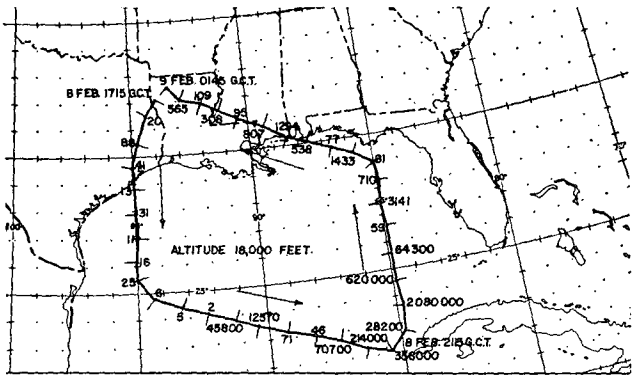


FIG. 49. Radioactivity observed on special flight over Gulf of Mexico on 8 February 1951. (Numbers give relative activity on "left" and "right" filters. Short dashes indicate points where filters were changed.)

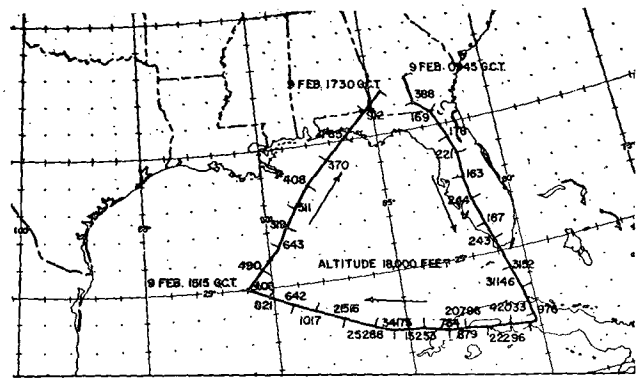


FIG. 50. Radioactivity observed on special flight over Gulf of Mexico on 9 February 1951. (For explanation, see fig. 49.)

## 5. Discussion of individual cases

The radioactivity observations in figs. 6 through 50 are presented for the use of the meteorologist. Comments in this article will be limited to only a few of the cases.

The flights were vectored on the basis of meteorological predictions. These predictions, of course, depended on the reported heights of the atomic clouds, and these were not always accurate. In the case of burst 3, on 1 February 1951, first reports of cloud height indicated that the debris had penetrated an inversion at 12,000 ft so that some of the debris would be transported eastward. Flights which were vectored to intercept this eastward moving debris failed to pick up any radioactivity. The embarrassment of the meteorologist was eliminated only after it was discovered that none of the cloud extended above 12,000 ft and all of it moved southward.

The trajectories of the atomic cloud from the fourth burst showed very little directional shear to the Gulf of Mexico (fig. 4). The 18,000-ft path is verified by the data on fig. 32, showing the most active filters of any of the flights of this series. However, when the same trajectory was carried eastward to the 80th meridian, the flight represented by fig. 27 intercepted no radioactivity in the predicted area (about 25°N). The small amount of radioactivity found north of 32°N is believed to be some residual activity from an earlier burst — certainly the magnitude of the peak on fig. 32 (almost 10,000,000 units) is much larger than that reported in fig. 27. The lack of debris was finally rationalized by arguing that the winds were even slower than those used for the after-the-fact trajectories which, in turn, were slower than those which were forecast and used for the vectoring operation. It was apparent that the lack of wind observations over the Gulf of Mexico reduced the accuracy of the trajectories over that area.

## REFERENCES

1. List, R. J., 1954: On the transport of atomic debris in the atmosphere. *Bull. Amer. meteor. Soc.*, **35**, 315–325.
2. Moore, C. B., J. R. Smith, and A. Gaalswyk, 1954: On the use of constant-level balloons to measure horizontal motions in the atmosphere. *J. Meteor.*, **11**, 167–172.